

## Electrolytes for sodium ion batteries: A short review

Archana Chandra\*, Angesh Chandra & R S Dhundhel

Shri Shankaracharya Institute of Professional Management and Technology, Raipur 492 015, India

*Received 4 July 2019; accepted 11 December 2019*

Synthesis routes and ion conduction phenomenon in sodium ion conducting solid electrolytes have been reported in the present chapter. The different experimental and theoretical tools have been explained for preparation and ion conduction mechanism of solid electrolytes. The working principle of some polymer electrolyte based conductors has been explained.

**Keywords:** Ion conducting electrolytes, Solution-cast method, Hot-press method, XRD, FTIR, DSC

### 1 Introduction

Sodium ion conducting solid electrolytes show great technological promises and these can be potentially used for solid state devices viz batteries, sensors, etc. Based on the wide availability and low cost of sodium, ambient temperature sodium-based batteries have the potential for meeting large scale grid energy storage needs<sup>1-3</sup>. In addition, since sodium is so abundant, sodium-based batteries could provide an alternative chemistry to lithium batteries and might become competitive to lithium-ion batteries in certain other markets. Supplies of sodium-containing precursors are vast with huge reserves of 23 billion tons of soda ash located in the United States alone. The abundance of resources and the much lower cost of trona (about \$135–165/ton) from which sodium carbonate is produced, compared to lithium carbonate (about \$5000/ton in 2010), provide compelling rationales for the use of sodium in large scale battery applications, particularly in the near-term<sup>4</sup>. Among the known ion conductors, Na<sup>+</sup> ion salt shows various advantage such as its availability in abundance at a cheaper cost than lithium and more softness of the material makes it easier to achieve good contact with electrode and electrolyte in the solid state devices viz polymeric batteries fabrication<sup>5-7</sup>. The interaction between other alkali ions and the polar groups of polymer is stronger than that of Na<sup>+</sup> ion. Thus, in lithium or other alkali ions, more activation energy required for ionic conduction than Na<sup>+</sup> ion in polymer electrolyte. Hence, the Na<sup>+</sup> ion salts can be selected as a dopant to prepare the ion conducting

solid electrolytes<sup>8</sup>. Technical characteristics of modern lithium-ion batteries have been approached their theoretical limits already. Whereas, the perspectives of their explosive development are thought of as problematic because of the scarcity of lithium natural resources and relatively low grade of lithium ores. On this reason, in these latter days the question arose on the devices that will replace the lithium-ion batteries. Among all candidates, the most often discussed devices are (i) lithium-air, (ii) lithium-sulphur, and (iii) sodium-ion batteries<sup>9</sup>. The most common electrolyte formulations for sodium batteries use either NaPF<sub>6</sub> or NaClO<sub>4</sub> as salts in carbonate ester solvents, particularly propylene carbonate (PC). Unfortunately, metallic sodium anodes corrode continuously in the presence of most commonly used organic electrolytes, rather than forming a stable solid electrolyte interphase (SEI). Highly reducing sodiated intercalation compounds intended for use as anodes may also require tailored SEIs to enable stable cycling in cells, similar to those that form on lithiated graphite electrodes in Li ion systems.

Typical reduction products as impurities such as sodium propyl carbonate are generated at Na anode surfaces in reaction with PC, the most common solvent used in Na batteries. This species can in turn be oxidized at the opposite cathode at top-of-charge thereby, limiting capacity utilization and causing coulombic inefficiency. Formulations and conditions needed for proper SEI formation will need to be co-developed with anode materials to ensure success in the field. For example, recently, fluoroethylene carbonate (FEC) has been observed to form a passivating film (0.7 V reductions) on both carbon and native metallic sodium anodes thereby stabilizing

\*Corresponding author  
(E-mail: archanachem.chandra@gmail.com)

the electrodes to further side reactions with solvents. Other additives, for instance, those used in Li-ion batteries such as vinylidene carbonate (VC), ethylene sulfite (ES), and trans-difluoroethylene carbonate (DFEC) were not effective, but improved cycling was seen for FEC at 10 vol. % for the carbon anode.

In the present review we have been discussing the different methods for synthesis and characterization of sodium ion conducting solid electrolytes.

## 2 Experimental Details

### 2.1 Sample preparation

There are many different methods for preparation of sodium ion conducting solid electrolytes. The most important methods are discussed below.

#### 2.1.1 Melt-quenching method

The oldest established method of producing an amorphous solid is to cool the molten form of the material quickly. The distinguishing feature of the melt-quenching process of producing amorphous material is that the amorphous solid is formed by the continuous hardening, (i.e., increase in viscosity) of the melt. In the present study, all the glass systems were prepared by the melt-quenching technique and the method of preparation is explained as follows. The starting materials used for the preparation of the present systems are of high purity. The chemical compositions of the different dopant concentrations are tabulated.

All the chemicals were weighed accurately using an electrical balance, grounded to fine powder and mixed thoroughly. The batches were melted in silica crucibles by placing them in an electrical furnace at required temperature ( $\sim 700^\circ\text{C}$ ) and a photograph showing the set of an electrical furnace is shown in Fig. 1. The melts were then poured on a polished brass plate and pressed quickly with another plate. The glasses thus, obtained were transparent. The colour of the glass samples depends upon the nature of the dopants.

#### 2.1.2 Solution-cast method

Composite polymer electrolyte films are generally obtained by simple casting procedure. The polymer is the host and the inorganic salts are dissolved in adequate reciprocal compositions in suitable solvents, (e.g., acetonitrile, methanol, ethanol, double distilled water, etc.). Appropriate amounts of the salt mixture of the chosen stoichiometry and PEO were separately dissolved in methanol, and the two solutions were then stirred together for approximately 24 h. The

solutions were prepared in such a way that a ratio of 1 gm of PEO to  $100\text{ cm}^3$  of solvent was maintained, and this was found to be optimum for casting purposes. Solvent was allowed for evaporation at room temperature. The thickness of the cast film was approximately  $100\text{--}200\ \mu\text{m}$ . The schematic illustration of the preparation procedure of polymer electrolyte film is shown in Fig. 2.

#### 2.1.3 Hot-press technique

Recently, a novel hot-press technique has been developed for casting CPE films. Hot-press technique has several procedural conveniences viz solution free/dry, least expensive, quicker procedure etc. than those of solution-cast method<sup>10,11</sup>. Firstly, the polymer electrolyte composition: PEO + different ion conducting salts, exhibiting highest ionic conductivity have been identified as first phase host matrix and this is known as solid polymer electrolytes (SPEs). For this purpose, dry powders of pure polymer and ion conducting salts in different salt concentrations (wt %) would be thoroughly mixed and heated  $\sim 75^\circ\text{C}$ , (well above the melting point of PEO) for



Fig. 1 – Schematic diagram of melt-quenched furnace.

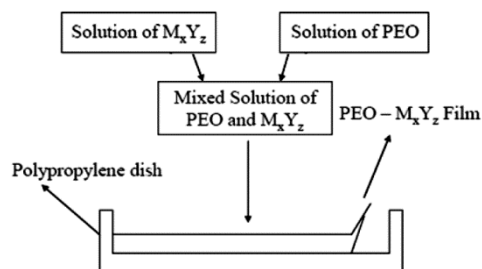


Fig. 2 – Schematic illustration of the preparation procedure of CPE films.

about 15 min to form the homogeneously mixed slurry. The slurry was then hot-pressed ( $\sim 1.25$  ton/cm<sup>2</sup>) between two SS blocks which ultimately resulted into mechanically stable membranes. On the basis of the salt-concentration dependent-conductivity measurements, the highest conducting composition have been identified and this have been used as first phase host for the dispersal of nano-sized inert materials viz SiO<sub>2</sub>, TiO<sub>2</sub>, Fe<sub>2</sub>O<sub>3</sub> etc. particles as second phase dispersoid. To prepare the composite polymer electrolytes (CPEs), we followed the same procedure, as mentioned above. Dry powders highest conducting composition were homogeneously mixed with different wt % ratios of nano-fillers, heated  $\sim 70$ - $80$  °C to form slurry, then hot-pressed between SS blocks resulting finally into a mechanically stable CPEs. In the present research laboratory a number of CPEs have been synthesized in this very quicker method.

#### 2.1.4 Solid solution reaction technique

Solid electrolytes can be synthesized by solid-solution reaction adopting following three routes of preparation:

Route 1: Sodium ion conducting solid electrolyte systems for example:  $x$  AgI:( $1-x$ ) NaI, where  $0.1 < x < 1$  mol wt (%), mixed homogeneously kept in separate silica test-tubes, heated at  $\sim 700$  °C (well beyond the melting temperatures of the constituent salts), shook the melt well for 15 min. then allowed to cool slowly in air to room temperature ( $\sim 27$  °C).

Route 2: The above mentioned homogeneously mixed molten compositions were kept at  $\sim 700$  °C for 48 h then cooled to room temperature as in route 1.

Route 3: The homogeneous mixtures in different compositions, as in route 1, were prepared by simple physical grinding at room temperature for 30 min.

The finished sample products were thoroughly ground, than pressed at  $\sim 4$  ton cm<sup>-2</sup> to form pallets of diameter  $\sim 1.28$  cm and thickness  $\sim 1$ - $3$  mm. The measurements of basic ionic transport parameters have been carried out on these sample pellets using different experimental techniques as discussed below.

#### 2.2 Material characterization techniques

Material characterizations of solid electrolytes were done with the help of following important techniques:

X-ray diffraction (XRD): X-ray diffraction (XRD) is an important experimental tool widely used to determine structures, identify materials phases as well

as materials characterization. When X-rays are scattered from the set of atomic planes of crystalline/polycrystalline solids, they interfere constructively by obeying the well-known Bragg's criterion:

$$2d \sin \theta = n\lambda \quad \dots (1)$$

Where,  $d$  is the inter-planer distance,  $\theta$  is the angle of incident of X-rays,  $n$  is an integer and  $\lambda$  is the wavelength of the incident X-rays.

Scanning electron microscopy (SEM): The scanning electron microscope (SEM) consists of well-defined, highly focused energetic beam of electrons. The beam is made to scan across the surface of the sample and is capable of producing high-resolution primary images of a sample surface as well as secondary electron imaging.

Fourier transform infrared (FTIR): Fourier transform infrared spectroscopy (FTIR) is a technique which is used to obtain an infrared spectrum of absorption, emission, photoconductivity or Raman scattering of a solid, liquid or gas. An FTIR spectrometer simultaneously collects high spectral resolution data over a wide spectral range. This confers a significant advantage over a dispersive spectrometer which measures intensity over a narrow range of wavelengths at a time.

Differential scanning calorimetric (DSC): Differential scanning calorimetry (DSC) techniques are used widely for thermal characterization of the materials. These studies provide quantitative/qualitative insights regarding the physical/chemical changes occurring in the materials during thermal cycling. This information are in term of endothermic/exothermic responses or change in heat capacity which corresponds to phase transition temperature ( $T_c$ ), glass-transition temperature ( $T_g$ ), crystallization temperature ( $T_p$ ), heat enthalpy, degree of amorphousity and/or crystallinity etc. of the sample material.

Thermogravimetric analysis (TGA): Thermogravimetric analysis (TGA) is a method of thermal analysis in which changes in physical and chemical properties of materials are measured as a function of increasing temperature (with constant heating rate), or as a function of time (with constant temperature and/or constant mass loss). TGA can provide information about physical phenomena, such as second-order phase transitions, including vaporization, sublimation, absorption, adsorption and desorption. Likewise, TGA can provide information

about chemical phenomena including chemisorptions, decomposition and solid-gas reactions, (e.g., oxidation or reduction). TGA is commonly used to determine selected characteristic of materials that exhibit either mass loss or gain due to decomposition, oxidation or loss of volatiles (such as moisture).

It is an especially useful technique for the study of composite polymeric materials, including thermoplastics, thermosets, elastomers, composites, plastic films, fibers, coatings and paints.

### 2.3 Ion transport characterization techniques

Ion transport characterization can be done with the help of following different ionic parameters:

#### 2.3.1 Conductivity measurement

Ionic conductivity ( $\sigma$ ) can be determined with the help of impedance spectroscopy (IS). The impedance spectroscopy (IS) is a powerful technique, used to evaluate the true bulk resistance ( $R_b$ ) of ionic/superionic materials for which dc conductivity measurements are normally avoided due to polarization effects. The ionic conductivity can be determined by the equation:

$$\sigma = \frac{l}{R.A} \quad \dots(2)$$

Where,  $l$  is the thickness and  $A$  is the cross sectional area of the polymeric film.

#### 2.3.2 Ionic mobility and ionic transference number measurement

The ionic mobility ( $\mu$ ) and ionic transference number ( $t_{ion}$ ) measurements can be carried out by dc polarization/depolarization studies using transient ionic current (TIC) method, as reported in our earlier communications<sup>12,13</sup>.  $\mu$ -values can also be directly evaluated using the time of flight ( $\tau$ ) data obtained from different 'transient ionic current-time' plots. The ionic mobility of CPEs can be determined at with the help of following equation:

$$\mu = \frac{d^2}{V.\tau} \quad \dots(3)$$

Where,  $d$  is the thickness of the samples,  $V$  is the applied external d.c. potential and  $\tau$  is the time of flight. The time of flight ( $\tau$ ) was determined directly employing dc polarization transient ionic current (TIC) technique. The schematic experimental arrangement for  $\mu$ -measurements using dc polarization TIC technique and a typical TIC plot is shown in Fig. 3. The mobile ion concentration ( $n$ ) was

evaluated at different temperatures from  $\sigma$  and  $\mu$  data by using the well-known relation:

$$\sigma = n. q. \mu \quad \dots(4)$$

Where,  $q$  is the charge. Ionic transference number ( $t_{ion}$ ) has also been evaluated at different temperatures using dc polarization technique with the help of following equation:

$$t_{ion} = 1 - \frac{I_e}{I_T} \quad \dots(5)$$

Where,  $I_e$  is the electronic current and  $I_T$  is the total current of the cell: [SS // CPE OCCs // SS].

#### 2.3.3 Ionic drift velocity measurement

The ionic drift velocity ( $v_d$ ) of the solid electrolytes can be evaluated at different temperatures using the following equation:

$$v_d = \frac{I_T}{A.n.q} \quad \dots(6)$$

Where,  $I_T$  is total current,  $A$  is the cross-sectional area of the film,  $q$  is the charge on the mobile ion. From temperature dependent ionic drift velocity studies, the energy involved in this thermally activated process was computed from 'log  $v_d - 1/T$ ' plot expressed by the equation:

$$\log v_d = \log v_{d0} \pm \exp(E_d / kT) \quad \dots(7)$$

## 3 Ion Conduction Phenomenon's

The ion conduction phenomenon of some sodium ion conducting solid electrolytes has been reviewed. Figure 4 shows the room temperature conductivity ( $\sigma$ )

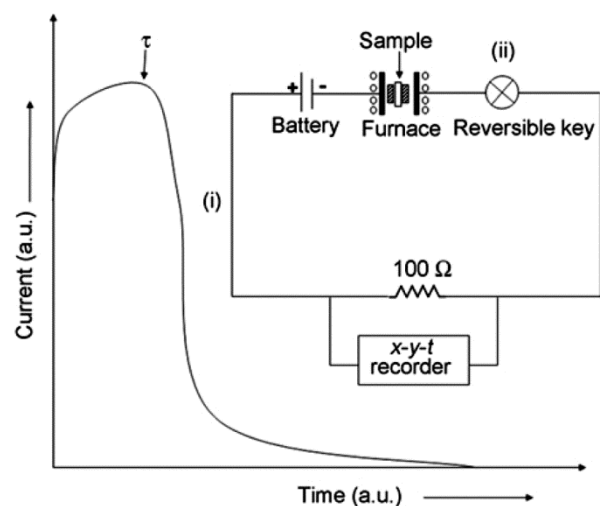
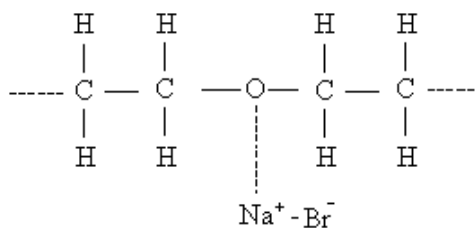


Fig. 3 – Schematic experimental arrangement used in TIC technique and some typical 'current versus time' plots.

variations for the sodium ion conducting solid polymer electrolytes (SPEs): (1-x) PEO: x NaBr, where  $0 < x < 50$  wt %. To determine the bulk resistance ( $R_b$ ), the impedance plot for highest conducting composition of SPE at room temperature is shown in bottom inset of Fig. 4. The conductivity increased when the ionic salt NaBr concentration increased initially from 0 to 30 wt % and then decreased on further addition of salts. The conductivity maxima appeared at  $x=30$ , i.e., the composition: (70PEO:30NaBr) with  $\sigma \sim 7.58 \times 10^{-7} \text{ Scm}^{-1}$ . This highest conducting composition has been referred to as optimum conducting composition (OCC). SPE films beyond 50 wt % salt concentration appeared, unstable and brittle. A conductivity increase of more than two orders of magnitude was obtained in SPE OCC from that of the pure PEO ( $\sigma \sim 3.2 \times 10^{-9} \text{ Scm}^{-1}$ ). The schematic representation of ion conduction in sodium ion conducting solid polymer electrolytes is shown in Fig. 5. The increase in

conductivity is due to the increase in degree of amorphousity and/or increase in ionic mobility ( $\mu$ )/mobile ion concentration ( $n$ ) which can be also be explained by the various models viz. mobility enhancement model, percolation model etc.<sup>13,14</sup>.

The possible configuration of newly synthesized hot-pressed SPE OCC is:



To explain the conductivity enhancement in the present SPE OCC again, the ionic mobility ( $\mu$ ) and mobile ion concentration ( $n$ ) studies have been done with the help of d.c. polarization transient ionic current (TIC) technique, as mentioned in experimental section. Figure 6 shows ‘log  $\mu$ -x’ and ‘log  $n$ -x’ plots for SPEs: (1-x)PEO: xNaBr. One can clearly notice the existence of maxima for both  $\mu$  &  $n$  at  $x=30$  wt % observed. This explains the fact that the overall increase in ionic conductivity of SPE OCC has been due to increase in both  $\mu$  &  $n$ .

Figure 7 shows the salt concentration dependent conductivity ( $\sigma$ ) for the hot-pressed solid polymeric electrolytes (SPEs): (PEO:NaClO<sub>4</sub>) at room temperature. Three orders of conductivity increased as the salt concentration increased. A moderate-sized  $\sigma$  - maxima ( $\sim 7.07 \times 10^{-7} \text{ S.cm}^{-1}$ ) was observed at 30 wt % of the salt NaClO<sub>4</sub>, [i.e., for the composition<sup>3</sup>:

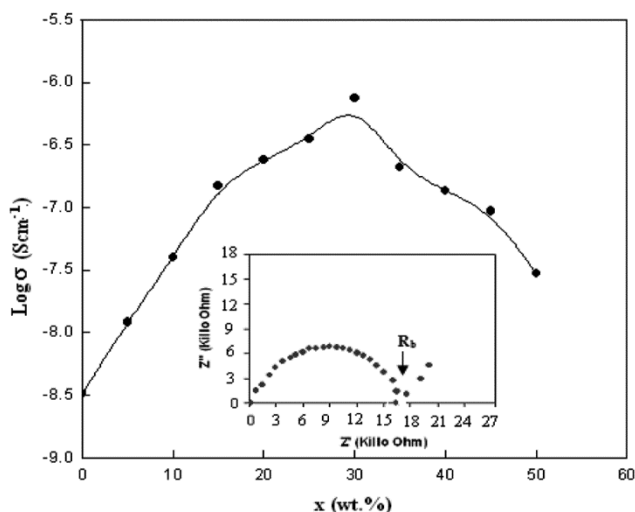


Fig. 4 – ‘Log  $\sigma$  - x’ plot of hot-pressed SPEs: (1-x)PEO: xNaBr. Bottom inset: Impedance plot for SPE OCC: [70PEO: 30NaBr]<sup>8</sup>.

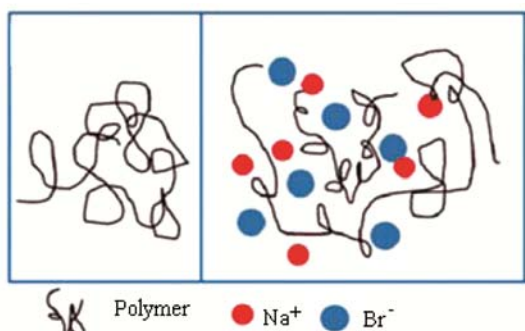


Fig. 5 – Schematic representation of ion conduction in sodium ion conducting polymer electrolytes.

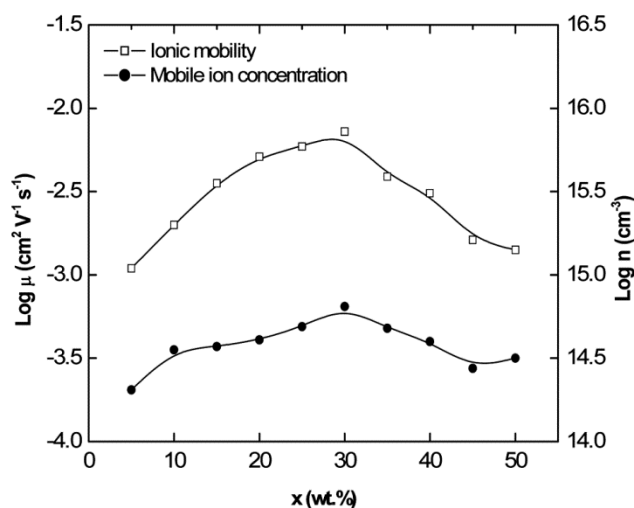


Fig. 6 – ‘Log  $\mu$  - x’ and ‘log  $n$ -x’ plots of hot-pressed SPEs: (1-x) PEO: xNaBr.

(70PEO: 30NaClO<sub>4</sub>). The addition of salt in PEO resulted into an increase in the degree of amorphicity/decrease in degree of crystallinity and number of mobile ions which in turn gave rise to an abrupt increase the conductivity in SPEs.

Figure 8 shows the filler SiO<sub>2</sub> dependent conductivity plot for nano-composite polymer electrolytes (NCPEs): (1-x) [70PEO: 30NaClO<sub>4</sub>] + x SiO<sub>2</sub> where x in wt (%). The ionic conductivity ( $\sigma$ ) of NCPE increases with increasing the concentration of nano-filler SiO<sub>2</sub> and one order of conductivity enhancement were observed from that of the pure SPE host: (70PEO: 30NaClO<sub>4</sub>). The two maximum conductivity values of  $7.6 \times 10^{-6}$  S/cm and  $5.12 \times 10^{-6}$  S/cm were observed at 7 wt % and 12 wt % of

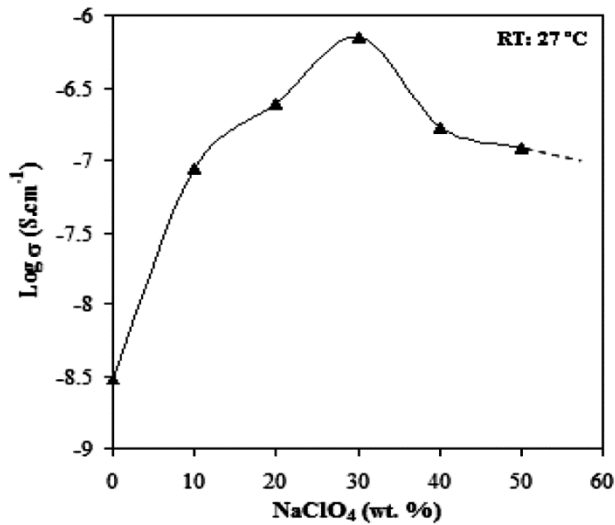


Fig. 7 – Room temperature conductivity plot<sup>3</sup> for SPEs: (PEO: NaClO<sub>4</sub>).

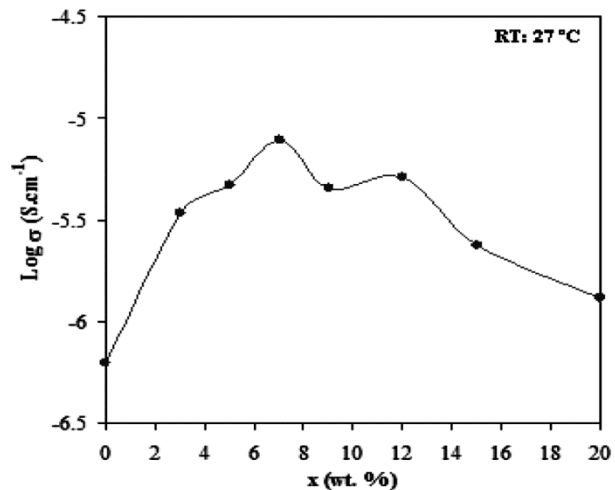


Fig. 8 – ‘Log  $\sigma - x$ ’ plot<sup>3</sup> for NCPEs: (1-x) [70PEO:30NaClO<sub>4</sub>] + x SiO<sub>2</sub>.

dispersal SiO<sub>2</sub>, respectively. However, the maximum conductivity of  $7.6 \times 10^{-6}$  S/cm has been observed at 7 wt % of SiO<sub>2</sub> and this has been referred to as optimum conducting composition (OCC). The existence of two peaks for the NCPEs has already been reported by several workers<sup>14,15</sup>. The existence of two  $\sigma$ -maxima in the present NCPEs can be attributed to two separate percolation thresholds involving two different kinds of mobile species: cation (Na<sup>+</sup>) and anion (ClO<sub>4</sub><sup>-</sup>). The ionic conductivity enhancement in NCPE is due to the creation of additional hopping sites and favorable conducting pathways for migrating ionic species through lewis acid-base reactions. In the present NCPE system, the following two types of cross linking are possible: (a) transient cross-linking of polymer segments via cation interaction and (b) transient cross-linking of polymer segments via cation-anion interaction is shown in Fig. 9

Figure 10 shows ‘log  $\sigma - 1/T$ ’ plot for the SPE films. The conductivity increased almost linearly with

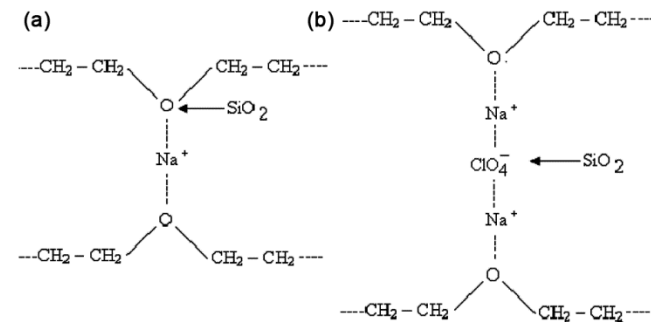


Fig. 9 – Schematic representation of two kind of cross-linking in polymer segments<sup>3</sup>.

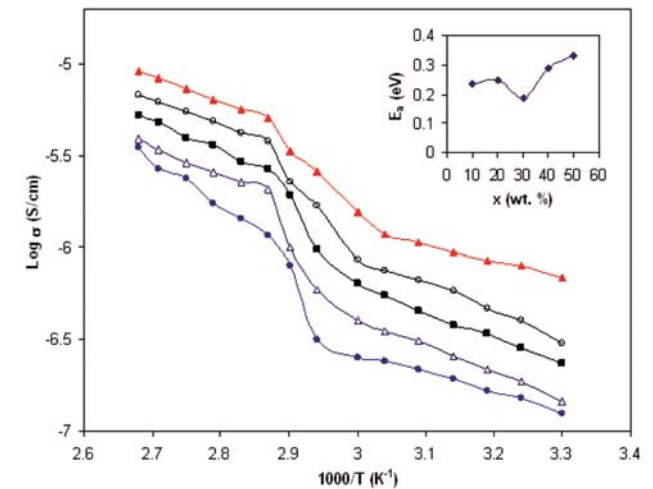


Fig. 10 – ‘Log  $\sigma - 1/T$ ’ plots for SPE films: (1-x) PEO: x NaHCO<sub>3</sub>, where x = 10 (●), 20 (○), 30 (▲), 40 (■), 50 (Δ). Top inset: ‘E<sub>a</sub> vs x’ plot<sup>16</sup>.

temperature up to  $\sim 70$  °C at which an upward jump in conductivity was observed<sup>16</sup>. The jump in conductivity at this temperature corresponds to semi-crystalline to amorphous phase transition of PEO. The linear portion of ‘log  $\sigma$  -1/T’ plots below  $T_m$  can be expressed by following Arrhenius equation:

$$\sigma = \sigma_o \exp (- E_a/kT) [\text{S.cm}^{-1}] \quad \dots(8)$$

Where,  $\sigma_o$  is the pre-exponential factor,  $E_a$  is the activation energy in eV and  $k$  is the Boltzmann constant. The  $E_a$  values, for all the compositions, were computed from linear least square fitting of the above equation, as shown the top inset in Fig. 10. The Arrhenius behavior of SPE OCC is given by the following equation:

$$\sigma(T) = 8.19 \times 10^{-4} \exp (- 0.185/kT) [\text{S.cm}^{-1}] \quad \dots (9)$$

It can be clearly noticed that for OCC SPE film with the activation energy  $E_a \simeq 0.185$  eV is lowest as compared to other SPE films. Low ‘ $E_a$ ’ is indicative of relatively easier ion migration in the hot-pressed solid polymer electrolyte film and this can be potentially used as electrolyte for electrochemical device applications.

#### 4 Conclusions

The preset short review successfully explained the different preparation routes for synthesis, and characterization of some sodium ion conducting electrolytes. The conductivity enhancements in some sodium ion conducting solid polymer electrolytes have also been explained. The sodium ion conducting electrolytes can be potentially used for solid state battery fabrication.

#### Acknowledgement

Author gratefully acknowledge to DST, New Delhi, for providing financial assistance through a project ‘Women Scientist Scheme – A’ (SR/WOS-A/CS-53/2018). We also gratefully acknowledge to CSVTU, Bhilai, for providing financial assistance through the ‘Collaborative research Project TEQIP-III’, (CSVTU/CRP/TEQIP-III/81/2019).

#### References

- 1 Laskar A L & Chandra S, *Superionic solids and solid electrolytes: Recent trends* (Academic Press Science, New York, 1981).
- 2 Chowdary B V R, *Solid state ionics: Advanced materials for emerging technologies* (World scientific publication, Singapore, 2006).
- 3 Chandra A, Chandra A & Thakur K, *European Phys J Appl Phys*, 69 (2015) 2090.
- 4 Michael D, Donghan K, Lee E & Christopher S, *Adv Funct Mater*, 23 (2013) 947.
- 5 Anantha P S & Hariharan K, *Solid State Ionics*, 176 (2005) 155.
- 6 Mohapatra S R, Thakur A K & Choudhary R N P, *Ionics*, 14 (2008) 255.
- 7 Kiran K K, Ravi M, Pavani Y, Bhavani S, Sharma A K & Narasimha V V R, *J Non-Crystalline Solids*, 358 (2012) 3205.
- 8 Chandra A, *Indian J Pure Appl Phys*, 54 (2016) 516.
- 9 Tarascon J M, *Phil Trans R Soc A*, 368 (2010) 3227.
- 10 Chandra A, *Eur Phys J Appl Phys*, 50 (2010) 21103.
- 11 Chandra A, *Indian J Pure Appl Phys*, 54 (2016) 583.
- 12 Chandra S, Tolpadi S K & Hashmi S A, *Solid State Ionics*, 28-30 (1988) 651.
- 13 Chandra A, Chandra A & Thakur K, *Arbian J Chem*, 9 (2016) 400.
- 14 Lakshmi N & Chandra S, *Phys Stat Sol (a)*, 186 (2001) 383.
- 15 Lakshmi N & Chandra S, *J Mater Sci*, 7 (2002) 197.
- 16 Chandra A, Chandra A & Thakur K, *Polymer Bull*, 71 (2014) 181.